

NASA Technical Memorandum 80068

NASA-TM-80068 19790016863

Capturing and Tracking Performance  
of the Horizontal Guidance and  
Control Systems of the Terminal  
Configured Vehicle

FOR REFERENCE

NOT TO BE TAKEN FROM THIS ROOM

Charles E. Knox

JUNE 1979

REF ID: A71

JUN 21 1979

LAWRENCE BERKELEY CENTER  
LIBRARY, 1979  
140 PTOM, VIBRANT



NF00554

1 Report No NASA TM-80068	2 Government Accession No	3 Recipient's Catalog No	
4 Title and Subtitle CAPTURING AND TRACKING PERFORMANCE OF THE HORIZONTAL GUIDANCE AND CONTROL SYSTEMS OF THE TERMINAL CONFIGURED VEHICLE		5 Report Date June 1979	6 Performing Organization Code
7 Author(s) Charles E. Knox		8 Performing Organization Report No L-11442	10 Work Unit No 513-52-01-16
9 Performing Organization Name and Address NASA Langley Research Center Hampton, VA 23665		11 Contract or Grant No	13 Type of Report and Period Covered Technical Memorandum
12 Sponsoring Agency Name and Address National Aeronautics and Space Administration Washington, DC 20546		14 Sponsoring Agency Code	
15 Supplementary Notes			
16 Abstract <p>A twin-jet commercial transport equipped with digital navigation, guidance, and control systems and advanced electronic display system was used for airborne operational research in the NASA Terminal Configured Vehicle Program. This report contains the results of flight tests which evaluated a second-order horizontal-path guidance control law and the autopilot and airplane response. This evaluation was accomplished through analysis of recorded flight data and through pilot opinion of the airplane maneuvers during automatic path-capture scenarios and path tracking. Four different path captures were flown at a ground speed of approximately 160 knots and repeated at approximately 300 knots. Path tracking error was measured in terms of cross track error along two paths: one path at cruise speeds and one at airport-terminal-area speeds. The path tracking accuracy and the smoothness of the airplane maneuvers were judged satisfactory for high speeds; however, at lower speeds the control law design should be improved so that tracking will be more accurate for operations in the airport terminal area.</p>			
17 Key Words (Suggested by Author(s)) Navigation Area navigation Autopilot		18 Distribution Statement Unclassified - Unlimited	
Subject Category 08			
19 Security Classif (of this report) Unclassified	20 Security Classif (of this page) Unclassified	21 No of Pages 30	22 Price* \$4.50

\* For sale by the National Technical Information Service Springfield Virginia 22161

NASA-Langley, 1979

**Capturing and Tracking Performance  
of the Horizontal Guidance and  
Control Systems of the Terminal  
Configured Vehicle**

Charles E. Knox  
*Langley Research Center  
Hampton, Virginia*



National Aeronautics  
and Space Administration

**Scientific and Technical  
Information Branch**

## SUMMARY

The NASA Terminal Configured Vehicle Program was established to examine the airborne aspects of advanced navigation and flight control systems and operational procedures for the fourth-generation air traffic control system. To accomplish the flight research of the program in a realistic manner, a twin-jet commercial transport airplane was equipped with a separate, full-scale research flight deck, located in the airplane cabin just forward of the wing; a digital navigation system; a digital guidance and control system; an advanced electronic display system; and an extensive data recording system. The digital navigation and guidance and control systems permit research and evaluation of various system concepts and control laws in an operational flight environment.

This report contains the results of the flight tests designed to evaluate a second-order horizontal-path guidance control law and to determine the autopilot tracking error during various automatic path capturing and tracking tasks. The control law evaluation was accomplished through analysis of recorded flight data and pilot opinion of the airplane maneuvers required to accomplish a prescribed task.

The horizontal path capture evaluation was accomplished while flying four different path captures, each with different initial conditions. Each path capture was flown at a ground speed of approximately 300 knots (cruise or high speed) and repeated at approximately 160 knots (close-in or low speed). The lateral-path-displacement and track-angle-error initial conditions were typical of those found during normal flight operations but were chosen so that particular characteristics of the control law could be observed.

Path captures at high speeds were judged by the pilots to be smooth and appropriate. However, at low speeds, the time required for the asymptotic capture was considered too long for close-in operations in the airport terminal area.

Path tracking and the autopilot tracking error were established on the autopilot flights along two programmed paths. Both of these paths required a high degree of maneuvering, one at cruise speeds and the other at close-in airport-terminal-area speeds.

The accuracy of path tracking and the smoothness of the airplane maneuvers were judged satisfactory for tracking at cruise speeds. However, for low speeds, the control law design should be improved so that tracking will be more accurate for close-in airport operations.

## INTRODUCTION

The NASA Terminal Configured Vehicle (TCV) Program was conceived to examine the compatibility of aircraft, advanced navigation and flight systems, and operational procedures in an advanced air traffic control system. The broad objectives of the TCV program include improving terminal area capacity and efficiency, improving approach and landing capability in adverse weather, and reducing noise through operational flight techniques. The TCV program will accomplish these objectives through analysis, simulation, and flight research.

The primary flight vehicle is a specially equipped, twin-jet commercial transport airplane. This airplane has been modified to include a separate, full-scale research flight deck, located in the airplane cabin just forward of the wing; a digital guidance and control system; a digital navigation system; an advanced electronic display (ref. 1); and an extensive data recording system. The digital navigation and guidance and control systems permit research and evaluation of various system concepts and control laws in an operational flight environment.

This report discusses the flight tests for the evaluation of a second-order horizontal-path guidance control law (ref. 2) and the horizontal guidance and autopilot path tracking error during fully automatic flight operation.

## SYMBOLS AND ABBREVIATIONS

CRT	cathode-ray tube
DME	distance measuring equipment
EADI	electronic attitude director indicator
$e_{ct}$	cross-track error, meters
EHSI	electronic horizontal situation indicator
$e_{ta}$	track-angle error, degrees
$g$	gravitational constant, 9.81 meters per second <sup>2</sup>
$K_y$	cross-track-error gain, 0.00902 degree per meter
$K_{\dot{y}}$	track-angle-error gain, 0.4593 degree per meter-second
$L$	course cut limit, degrees
NCU	navigation control unit
$r$	radius, meters
$r_t$	turn radius, $v_g^2/g \tan \phi$ , meters

$V_g$	ground speed, meters per second
$\gamma$	flight-path angle, degrees
$\phi$	bank angle, degrees
$\psi_I$	path intercept angle, degrees

#### DESCRIPTION OF AIRPLANE AND EXPERIMENTAL SYSTEMS

The test airplane is the TCV Boeing 737 research airplane (a twin-jet commercial transport) shown in figure 1. Although the airplane is used as an experimental vehicle, all normal flight systems (flight control, electrical, pressurization, etc.) and the conventional cockpit have been retained in a normal functional state. This retention of functions allows changes to occur to the experimental systems without affecting the operational safety of the airplane.

The experimental systems consist of a digital guidance and control system, a digital navigation system, and an electronic CRT display system integrated into a separate research flight deck. The research flight deck is full-scale and located in the airplane cabin just forward of the wing.

Figure 2 shows the research flight deck instrument panel. Each of the research pilots has three CRT displays for airplane attitude and navigation information. The EADI display provides the pilot with basic airplane altitude, flight-path angle, potential flight-path angle, and, at the pilot's discretion, flight director and navigation situation information. The EHSI display provides the pilot with an electronically drawn map of pertinent navigation information (routes, terrain, etc.) relative to the position of the airplane. The pilot may display other information such as other airports, obstacles, route altitudes and ground speeds, and airplane horizontal-path prediction information. The third CRT display is an input/output display for the NCU which is used to assist the pilots with flight planning and navigation.

#### Horizontal Guidance System

Figure 3 is a simplified functional block diagram of the experimental navigation, guidance, and control systems on the airplane. Various navigation sensors, including DME and inertial navigation system accelerations and velocities, are input to the navigation and guidance computer (a general purpose, digital processor). The navigation and guidance computer generates horizontal guidance commands based on its estimate of airplane position, velocity, and tracking errors from the programmed path. These input commands include cross-track error ( $e_{ct}$ ), ground speed ( $V_g$ ), and track-angle error ( $e_{ta}$ ) as shown in figure 4. The horizontal guidance commands are computed and transferred to the flight control computer at a rate of 20/sec. The output of the flight control computer then becomes the input to the servos for the control surfaces (ailerons, elevator, etc.).

Figure 5 is a block diagram of the horizontal guidance control law. The horizontal guidance control law was designed by assuming the airplane to be a simple, point mass, second-order system. (See ref. 2.) Cross-track error, track-angle error, and ground speed are combined to give a commanded lateral acceleration, in the form of a bank angle command proportional to the horizontal guidance errors. For all practical purposes, lateral acceleration is equal to  $g \tan \phi$  with coordinated turns assumed (i.e., no sideslip). During curved path segments, the nominal bank angle required to track the curved path with no wind and no horizontal-path error at the present ground speed of the airplane is added to the bank-angle command.

A course cut limit  $L$  was applied to the cross-track bank-angle command input when the airplane was a long distance from the horizontal path. The limit was a function of  $V_g$ ,  $K_y$ , and the desired  $\psi_I$  as

$$L = \frac{V_g K_y}{57.3} \psi_I \text{ deg}$$

If the cross-track command input was not limited by  $L$ , it would be significantly larger than the command input from track-angle error; this would cause the airplane to be flown in a circle, never intercepting the path. When  $L$  is applied, the airplane will be turned toward the path to an intercept angle  $\psi_I$ .

Figure 6 shows  $\psi_I$  as a function of cross-track error expressed in terms of turn radii ( $r_t = V_g^2/g \tan 20^\circ$ ). When the airplane has a cross-track error greater than  $3r_t$ , the airplane flies toward the path so that  $\psi_I = 90^\circ$ . The angle  $\psi_I$  decreases linearly from  $90^\circ$  to  $30^\circ$  as the cross-track error decreases from  $3r_t$  to  $1.5r_t$ . The  $\psi_I$  schedule is expressed mathematically as

$$\psi_I = \begin{cases} 30^\circ & (x < 30^\circ) \\ 90^\circ & (x > 90^\circ) \\ x & (\text{Otherwise}) \end{cases}$$

where

$$x = \frac{142.77 |\epsilon_{ta}|}{V_g^2} - 30 \text{ deg}$$

A  $30^\circ$  intercept angle will be held until an asymptotic path capture is started. Asymptotic capture starts when the cross-track error becomes less than the course cut limit divided by the cross-track-error gain  $L/K_y$ . During the asymptotic capture, the selected horizontal control law gains result in a

natural frequency  $\omega_n$  of 0.039 rad/sec where

$$\omega_n = \left( \frac{gK_y}{57.3} \right)^{1/2}$$

and result in a damping ratio  $\zeta$  of 1 where

$$\zeta = \frac{K_y}{2} \left( \frac{g}{57.3K_y} \right)^{1/2}$$

During the flight tests,  $K_y$  and  $K_{\dot{y}}$  were held constant at 0.009022 deg/m and 0.4593 deg/(m-sec), respectively. Since the cross-track-error gain and the track-angle-error gain were held constant during all speed ranges of flight, the capture and tracking characteristics were expected to be different at high (cruise) and low (airport terminal area) speeds. Hence, it was necessary that evaluation flights be conducted at both high and low speeds.

All inputs to the horizontal path control law were referenced to the ground rather than to an air-mass reference (i.e., ground speed rather than air-speed and track angle rather than airplane heading). As a result, the control law commanded the airplane to fly on a desired ground track regardless of wind effects.

The horizontal control law had no bank-angle feedback terms. Therefore, if the airplane was laterally or directionally mistrimmed so that a bank angle of  $n$  deg resulted when stabilized, the airplane would turn off the programmed path until a bank angle command of  $n$  deg in the opposite direction leveled the wings. This resulted in a constant lateral offset of  $n/K_y$  (110.8 m/deg of mistrim) from the desired path.

Lateral path offsets due to small bank-angle mistrimms, such as those resulting from asymmetrical thrust or fuel imbalance, were not readily detectable by the flight crew from the CRT map display. A 120-m offset (approximately  $1.1^\circ$  bank angle mistrim) on a map with a 4 n. mi./in. scale is less than 0.038 cm (0.015 in.). As a result, the flight crew was unaware of the lateral offset and did not retrim the airplane.

#### Data Acquisition System

Data were recorded onboard the airplane by a wide-band magnetic tape recorder at 40 samples/sec. These data included 93 parameters describing the airplane configuration, attitude, and control surface activity and 32 selectable

parameters from the navigation computer. In addition, video recordings of the EADI and the EHSI displays were made throughout the flight.

#### TEST CONDITIONS AND PROCEDURES

##### Horizontal Path Capture Tests

Four sets of capture conditions, with different initial cross-track errors and track-angle errors (path intercept angles), were flown to evaluate the horizontal-path capture characteristics. Each of the four captures were performed at ground speeds of approximately 160 knots and 300 knots.

Pilot opinion was used to evaluate, on the basis of ride comfort and normal operational standards, the smoothness and acceptability of the capture maneuver from the viewpoint of a pilot rather than a passenger. In their evaluations, the pilots considered bank angle, path intercept angle, path capture time (as functions of initial  $e_{ct}$  and  $V_g$ ), as well as the type of flight environment (cruise or terminal area). Recorded flight data were used to check that the airplane flew as commanded by the navigation and guidance computer.

The following table summarizes the initial conditions for each of the path capture tests:

Test condition	Initial conditions for -	
	$e_{ct}$	$\psi_I$
First	0.2 $r_t$	10° away from path
Second	0.20 $r_t$	70° toward path
Third	1.95 $r_t$	90° toward path
Fourth	4.0 $r_t$	179° toward path

Each set of these initial conditions was chosen to observe specific capture characteristics but was also typical of those found in normal operations.

The first horizontal-path-capture test condition was designed to evaluate the capture characteristics when the autopilot was engaged when the airplane had small cross-track and track-angle errors. The expected response from the autopilot was a turn toward the path for an asymptotic capture.

The second and third horizontal-path-capture test conditions were designed to evaluate the capture characteristics when the airplane was flying almost directly toward the path during autopilot engagement. In the second test condition, the autopilot was not engaged until the airplane was very close to the path, thus forcing the airplane to overshoot the path. In the third test condition, the autopilot was engaged in time for the airplane to capture the path without an overshoot. In both test conditions, the expected response from the

autopilot was to turn the airplane quickly toward a less than 30° intercept angle, followed by a gentler asymptotic capture.

The fourth horizontal-path-capture test condition was designed to evaluate the course cut limit  $L$  throughout its entire range. The autopilot was engaged when the airplane had a very large cross-track error and a path intercept angle of almost 180°. The expected response from the autopilot was to turn the airplane toward a 90° intercept angle until  $3r_t$  away from the path. Then the autopilot would turn the airplane to follow the,  $\psi_I$  schedule (fig. 6) until an asymptotic capture could be started.

#### Horizontal Path Tracking Tests

Two programmed flight paths were used to establish the horizontal-path autopilot tracking error. The autopilot tracking error was quantified by calculating the mean and the standard deviation of the cross-track error. The mean and the standard deviation of the cross-track error were calculated for the entire path and for each individual segment of the path. The airplane was allowed to stabilize on each segment of the path before the cross-track mean and the standard deviation were calculated for the individual segments.

Paths that required a series of maneuvers, instead of a straight and level path, were used during the tracking tests so that an upper limit on the autopilot tracking error could be obtained. The two paths used during the tracking tests, shown in figures 7 and 8, consisted of 17 either straight or curved segments defined by way points with different programmed altitudes and ground speeds. Programmed altitudes and ground speeds typically used during enroute flight (cruise) were used for path A, and those typically used during airport terminal area flight were used for path B.

The pilots were asked to evaluate the smoothness and acceptability of the maneuvers required to track the path, including transitions between the path segments. The pilot evaluations were based on the airplane pitch and roll attitude and on the autothrottle and control activity as a function of the ground speed and flight environment (cruise or terminal area).

### RESULTS AND DISCUSSION

#### Horizontal Path Capture

The data (fig. 9) for the first horizontal-path-capture test condition show that the airplane had an initial ground speed of 308 knots, an initial cross-track error of 964 m (0.14 $r_t$ ), and an initial track-angle error of 9.5° away from the path. After the autopilot was engaged, the airplane turned toward the path to a maximum intercept angle of 8° followed by a gradual reduction as the cross-track error became smaller. When the bank angle, cross-track error, and track-angle error stabilized, the test was completed. As shown in the figure, path capture was complete approximately 2 min after engaging the autopilot.

The first horizontal-path-capture test condition was repeated for the low ground speed capture. The data (fig. 10) show that when the horizontal path capture was started, cross-track error was 400 m ( $0.19r_t$ ) left of the path, track-angle error was  $10^\circ$  away from the path, and ground speed was 167 knots. The airplane then turned toward the path to a maximum intercept angle of  $6^\circ$ . The airplane converged to the path with a 30-m lateral offset. Path capture was achieved approximately 2 min after the autopilot was engaged. Atmospheric turbulence was encountered during several of the tests at low altitudes as indicated by the bank angle traces; winds were approximately 20 knots and gusty. However, no adverse effects were noted during the tests or on the cross-track-error and track-angle-error traces.

The second horizontal-path-capture test condition was first used for the high-speed capture. The data (fig. 11) show that the initial cross-track error was 1530 m ( $0.21r_t$ ), track-angle error was  $71^\circ$  toward the path, and the ground speed was 310 knots. After the horizontal path mode was engaged, the airplane rolled to a steady  $26^\circ$  bank angle to reduce the intercept angle. Although the final bank-angle command from the navigation computer was limited to  $25^\circ$ , an airplane mistrim would cause a small bank-angle bias to occur about the commanded bank angle. The large initial path intercept angle and small initial cross-track error designed in the second horizontal-path-capture test condition forced the airplane to overshoot the path by 3090 m (approximately  $0.44r_t$  at 308 knots) before turning toward the path. After the overshoot occurred, a maximum path intercept angle of  $19^\circ$  toward the path was gradually reduced as the cross-track error was decreased for the final path capture. The airplane converged to a 120 m lateral offset approximately 3.5 min after the horizontal path mode was selected.

The second horizontal-path-capture test condition was repeated at a lower ground speed. The data (fig. 12) show that the airplane had an initial ground speed of 158 knots, a cross-track error of 406 m ( $0.22r_t$ ), and a track-angle error of  $67^\circ$  toward the path. The airplane immediately rolled to a  $26^\circ$  bank after the horizontal path mode was engaged. A maximum overshoot of 1026 m ( $0.48r_t$  at 170 knots) occurred before the airplane could turn back to recapture the path. A maximum path intercept angle of  $11^\circ$  was used to recapture the path. The path capture was completed approximately 2.5 min after the horizontal path mode was selected.

Figure 13 shows the data for the third horizontal-path-capture test condition with the airplane flown at cruise speed. When the test was started, the airplane had a cross-track error of 12 660 m ( $2.0r_t$ ), a track angle error of  $90^\circ$ , and a ground speed of 292 knots. After the horizontal path mode was engaged, the airplane rolled to a  $24^\circ$  bank angle. This bank angle was maintained until the path intercept angle of the airplane was reduced to about  $45^\circ$ . Then the bank angle was gradually reduced to wings level with a resulting path intercept angle of  $27^\circ$ . The  $27^\circ$  intercept angle was held constant by the course cut limit until the cross-track error was 3325 m ( $0.50r_t$  at 298 knots). Then an asymptotic capture was started and the airplane converged to a lateral offset of 85 m at the completion of the capture. The asymptotic portion of the capture was completed in approximately 2.5 min. (Note that the previous capture tests referred to total time to capture the path.)

Figure 14 shows the data for the third horizontal-path-capture test condition for the low-speed capture. The test was started with a cross-track error of 3490 m ( $2.0r_t$ ), a track-angle error of  $87^\circ$  toward the path, and a ground speed of 155 knots. After the horizontal path mode was selected, the airplane rolled to a  $25^\circ$  bank angle followed by a quick reduction to  $8^\circ$ . This bank angle was gradually reduced toward wings level during the asymptotic capture. The asymptotic capture was started when the cross-track error was 2180 m ( $1.2r_t$  at 157 knots) and was completed in approximately 3 min. The initial roll to a  $25^\circ$  bank angle was caused by the course cut limit. When the cross-track error became less than  $1.2r_t$ , the bank angle was reduced for an asymptotic capture.

Figure 15 shows the data for the fourth horizontal-path-capture test condition conducted at high speed. The plots start where indicated and follow the direction of the arrows. The data show that the initial conditions were a cross-track error of 44 200 m ( $4.1r_t$ ), a track-angle error of  $176^\circ$  (almost parallel to the path but in the opposite direction), and a ground speed of 383 knots. When the horizontal path mode was selected, the airplane rolled to a  $25^\circ$  bank angle, turning toward the path. Bank angle roll-out to wings level was completed and the airplane stabilized on a path intercept angle of  $90^\circ$  as defined by the  $\psi_I$  schedule. When the cross-track error was 26 200 m ( $3r_t$  at 343 knots), the course cut limit caused the airplane to turn toward a  $30^\circ$  path intercept angle. The airplane then rolled to wings level on a  $30^\circ$  intercept angle at a cross-track error of 11 000 m ( $1.3r_t$  at 339 knots). This intercept angle was held until the asymptotic capture was started at a cross-track error of 4450 m ( $0.52r_t$  at 338 knots). Asymptotic capture was complete in approximately 2.5 min. Ground speed varied for the fourth horizontal-path-capture test condition because of the high winds and the airplane heading change of approximately  $180^\circ$ . However, no adverse effects on the capture tests were noted in the data.

Figure 16 shows the data for the fourth horizontal-path-capture test condition flown at low speed. The initial conditions for this test were a cross-track error of 16 800 m ( $7.2r_t$ ), a track-angle error of  $175^\circ$ , and a ground speed of 177 knots. After the horizontal path mode was selected, the airplane rolled to a  $25^\circ$  bank angle, turning toward the path to a  $90^\circ$  intercept angle. At a cross-track error of 3700 m ( $3r_t$  at 129 knots), the course cut limit caused the airplane to bank to a  $6^\circ$  angle and turn toward a  $30^\circ$  intercept angle. As the  $30^\circ$  path intercept angle was approached, the airplane started an asymptotic capture. The asymptotic capture took approximately 2 min from start to completion.

The pilots believed that the ride qualities during the horizontal captures were satisfactory at both high and low speeds. The  $\psi_I$  schedule was also adequate during the high- and low-speed captures. The asymptotic portion of the capture was adequate for high speeds, but the pilots believed that they would have captured the path more quickly if they had flown the airplane manually during the low-speed captures, particularly for close-in airport operations such as on the final approach to landing.

Horizontal captures at the lower speeds may be quickened by increasing the control law gains  $K_y$  and  $K_{\dot{y}}$ . However, the magnitude of these constant gains were limited by acceptable ride qualities, path capture characteristics, and control surface activity for high-speed flight.

One possible solution of the gain selection problem is to provide gains varied as a function of speed. This solution could result in satisfactory ride qualities and path capture characteristics at both high and low speeds. Time did not, however, permit data collection with variable gains.

#### Horizontal Path Tracking

The autopilot tracking error was expressed in terms of the cross-track error. Three flights were flown in the automatic path tracking mode: two flights on path A (typical cruise speeds) and one flight on path B (typical terminal area speeds). The mean and the standard deviation of the cross-track error for each of the flights and for 15 segments of path A and 12 segments of path B are presented in figures 17, 18, and 19.

Cross-track-error data are not presented for segments A6-A7 and A17-A18 of path A nor for segments B4-B5, B5-B6, and B6-B7 of path B. Segments A6-A7, A17-A18, and B6-B7 were turns designed to observe the system operation at the maximum bank-angle command of 25°. Thus, wind could drift the airplane away from the path if a bank angle greater than 25° was required for the airplane to fly on the path. Tracking data were not used following these turns until the airplane had again stabilized on the path. Segments B4-B5 and B5-B6 of path B are not presented because of a path definition error in the navigation computer.

The mean and the standard deviation of the cross-track-error data for each segment of the path were not calculated until the airplane was stabilized on track after passing each way point. Stabilization typically occurred within 15 sec after passing the way point. The mean and the standard deviation for the entire flight did, however, include the segment transitions.

Figures 17 and 18 show the mean and the standard deviation of the cross-track error for flight 1 and flight 2, respectively, for each segment of path A. The mean error was less than 200 m and the standard deviation less than 50 m for each of the segments. The mean and the standard deviation for the entire flight were 104 m and 69 m for the first flight and 20 m and 75 m for the second flight. The mean and the standard deviation of the cross-track error for path B are shown in figure 19. The mean was less than 145 m and the standard deviation was less than 89 m for each leg. For the entire flight, the mean and the standard deviation were 59 m and 54 m, respectively.

The cross-track error was typically nonoscillatory on each segment. The airplane would fly to a constant path offset and stabilize with the wings level and a zero track-angle error. On the longer path segments, such as A11-A12 of path A and B3-B4 of path B, this small cross-track error resulted in a lower standard deviation and a mean error approximately equal to the offset. A larger standard deviation on some of the shorter path legs, such as A14-A15 and B14-B15, was caused by a large change to the cross-track error along a short path leg.

The constant path offset was characteristic of a lateral airplane mistrim, possibly resulting from a fuel imbalance or asymmetric thrust setting. The off-

set effects could be reduced by modification of the control law. Two possible modifications would be to increase the control law gains or to add a forward path integrator; however, neither of these modifications was tested at this time.

Pilot comments indicated that the cross-track error on the cruise speed path was satisfactory for operations in the environment of today. The roll maneuvers required to maintain the path resulted in what the pilots considered to be a smooth ride. Horizontal path tracking error at the approach (low) speeds was satisfactory for terminal area maneuvering but could be too large for close-in airport operations such as on the final approach to landing. The pilots believed that they would have flown the airplane manually with higher roll rates and larger bank angles; thereby, less cross-track error would have resulted on the final approach.

#### CONCLUDING REMARKS

Path captures at high speeds were judged to be smooth and satisfactory from a piloting viewpoint. However, at the lower speeds, the time required for the asymptotic capture was considered to be too long for close-in airport operations such as during an approach to landing.

Path tracking error was determined on autopilot flights along two programmed paths. Each of these paths, one at cruise speeds and the other at near-airport-terminal-area speeds, required a high degree of maneuvering.

The path tracking error (cross-track error) mean was 104 m and its standard deviation 69 m for the cruise speed (path A) flights and 59 m and 54 m for the terminal area speed (path B) flight. The path tracking accuracy and the smoothness of the airplane maneuvering were judged satisfactory for tracking at cruise speeds. However, at lower speeds, the control law design should be improved so that tracking will be more accurate.

Langley Research Center  
National Aeronautics and Space Administration  
Hampton, VA 23665  
May 4, 1979

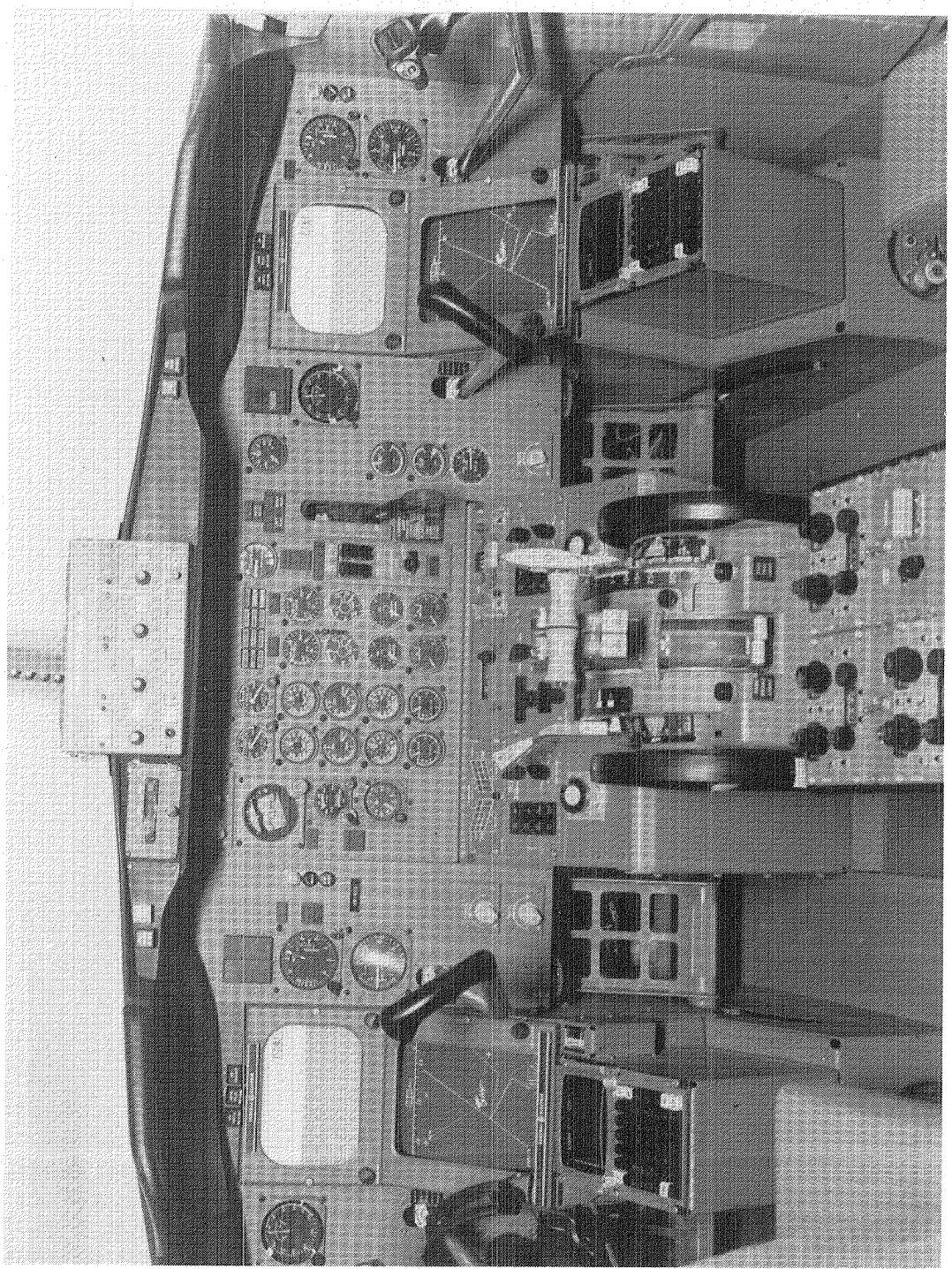
#### REFERENCES

1. Cosley, D.; and Martin, A. J.: ADEDS Functional/Software Requirements. SST Technology Follow-On Program - Phase II. Rep. No. FAA-SS-73-19, Dec. 1973. (Available from DDC as AD B000 287.)
2. McKinstry, R. Gill: Guidance Algorithms and Non-Critical Control Laws for ADEDS and the AGCS. Doc. No. D6-41565, Boeing Co., 1974.



L-73-6281

Figure 1.- TCV research airplane.



L-74-5183

Figure 2. - Research flight deck.

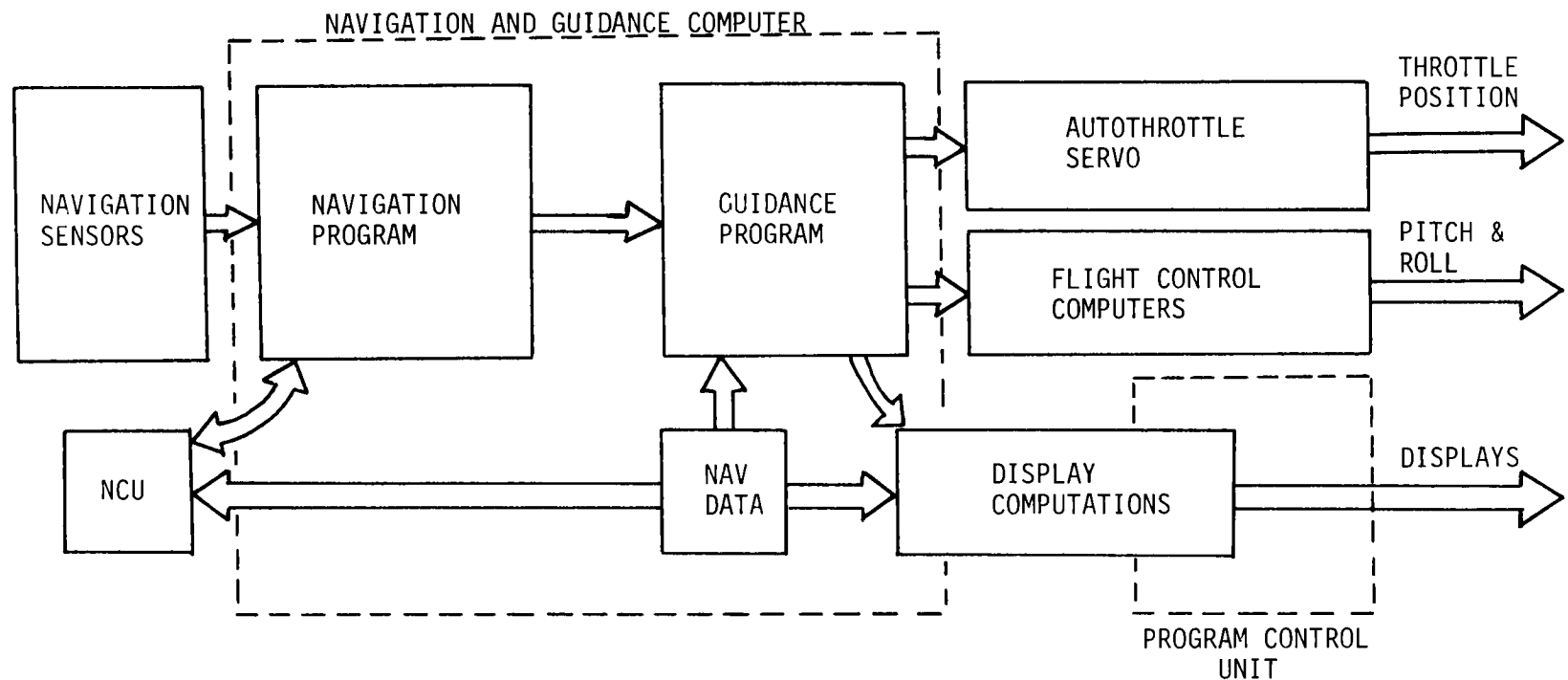


Figure 3.- Functional block diagram of navigation, guidance, and control systems.

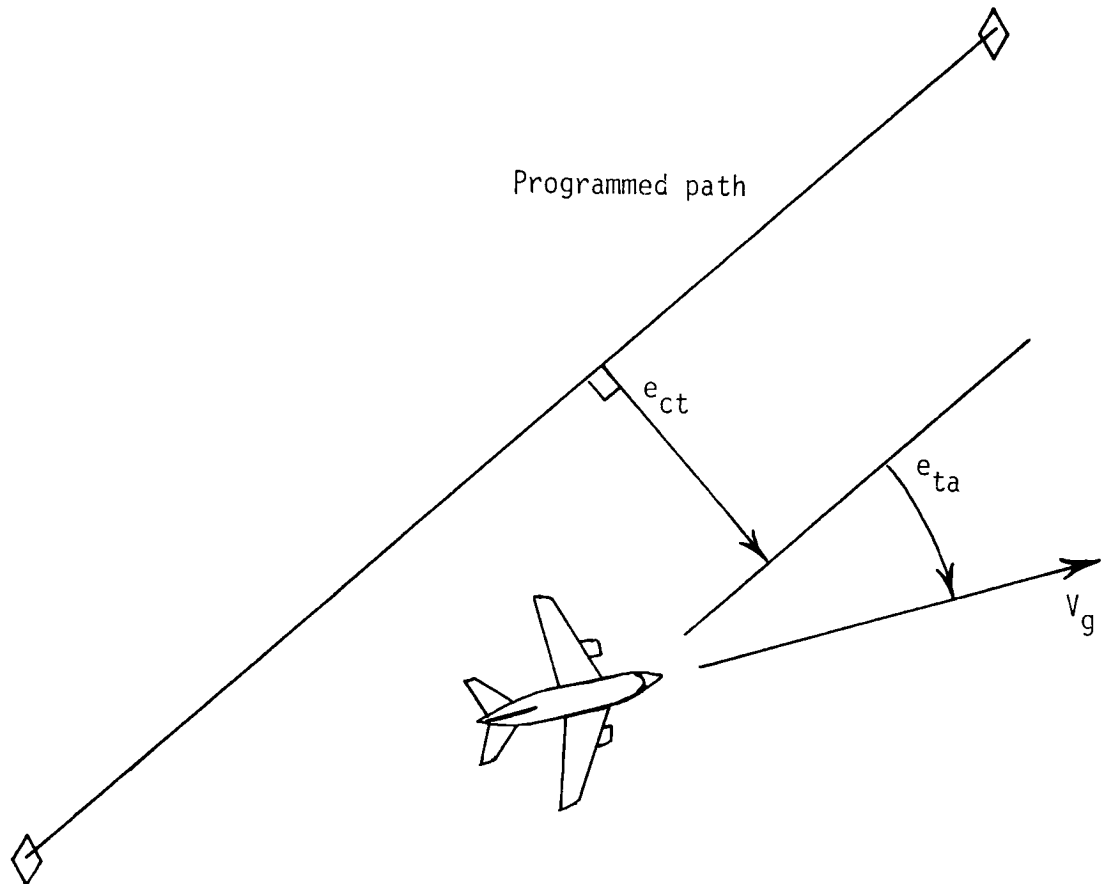


Figure 4.- Horizontal guidance input parameters. Positive directions are indicated by arrows.

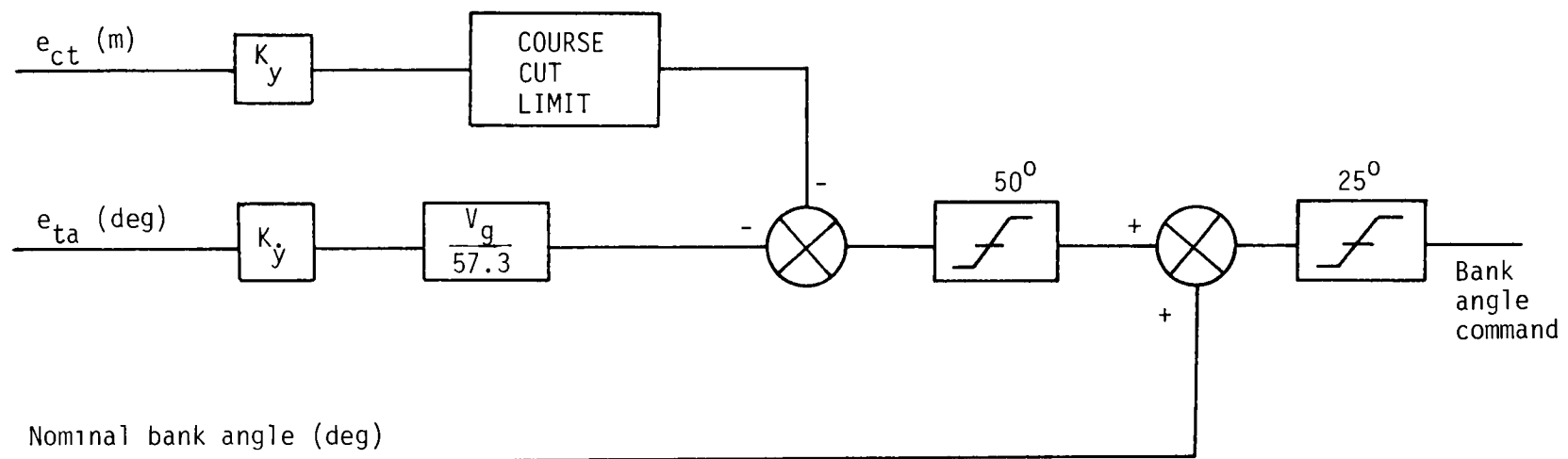


Figure 5.- Block diagram of horizontal guidance control law,  
 $K_y = 0.009022 \text{ deg/m}$ ;  $K_{\dot{y}} = 0.4593 \text{ deg/(m-sec)}$ .

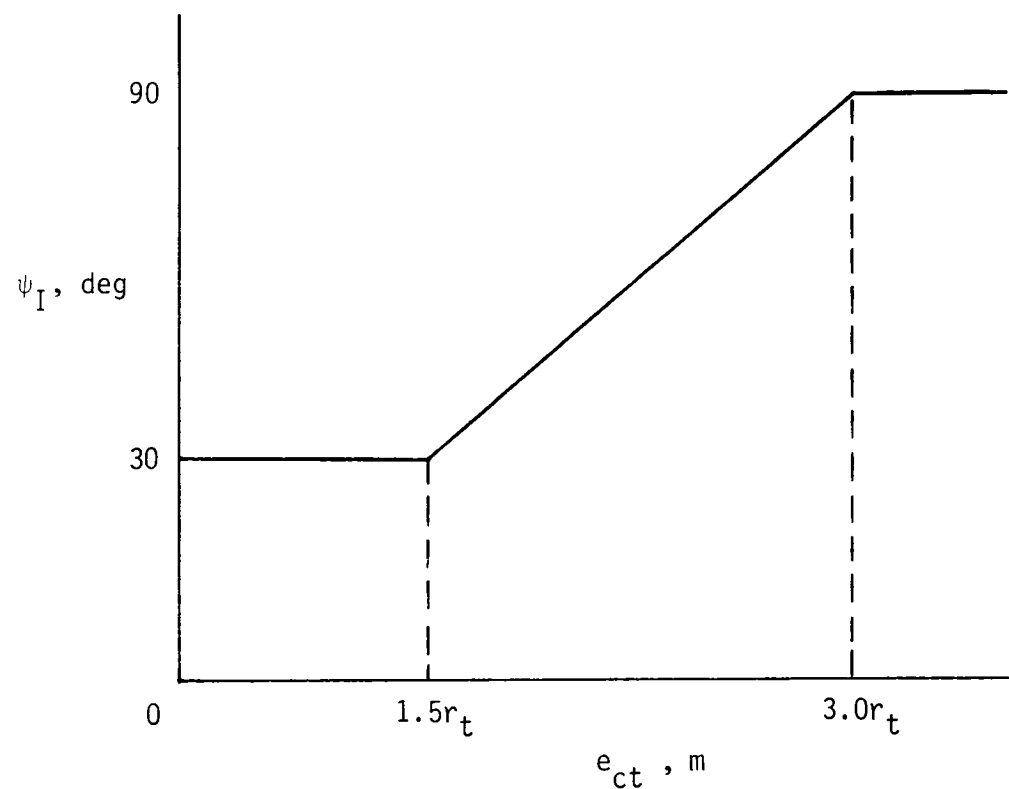


Figure 6.- Path intercept angle schedule.

Way point	$\gamma$ , deg	Altitude, m	Ground speed, knots	Way point	$\gamma$ , deg	Altitude, m	Ground speed, knots	Way point	$\gamma$ , deg	Altitude, m	Ground speed, knots
A1	0	1829	330	A7	0	4267	370	A13	-0.8	6096	380
A2	3.5	1829	330	A8	0	4267	330	A14	-2	5486	360
A3	0	5486	330	A9	0	4267	350	A15	1.6	3962	360
A4	0	5486	330	A10	0	4267	350	A16	0	5182	380
A5	0	5486	330	A11	0	4267	330	A17	2	5182	370
A6	-2.8	5486	370	A12	-0.9	6706	400	A18		6096	380

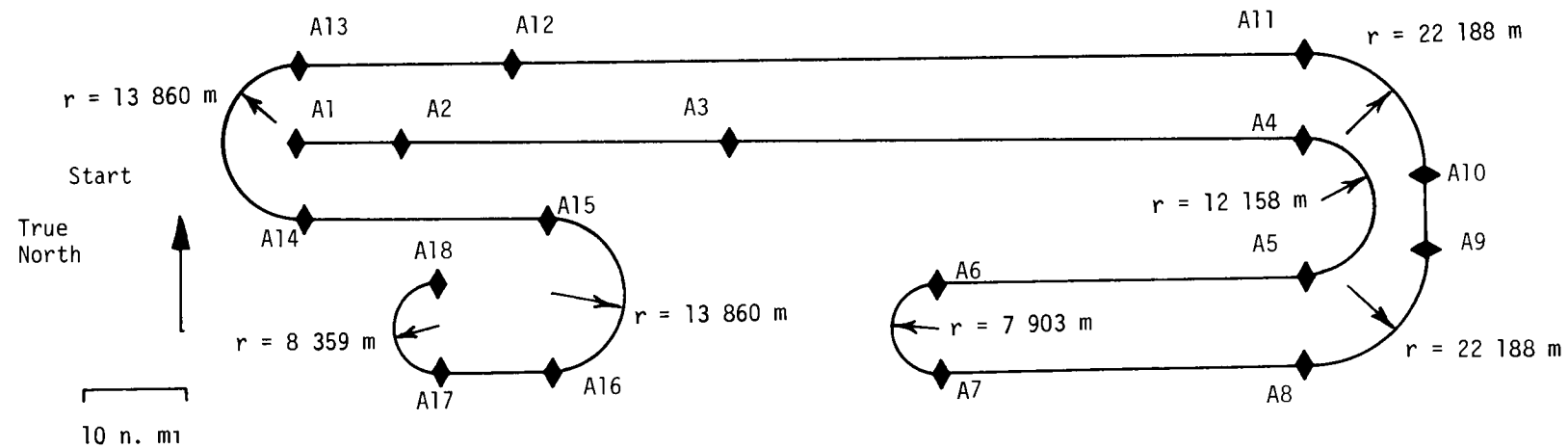


Figure 7.- Path A for tracking evaluation at cruise speeds.

Way point	$\gamma$ , deg	Altitude, m	Ground speed, knots	Way point	$\gamma$ , deg	Altitude, m	Ground speed, knots	Way point	$\gamma$ , deg	Altitude, m	Ground speed, knots
B1	0	610	160	B7	0	1372	175	B13	-6	1372	160
B2	3.5	610	160	B8	0	1372	160	B14	0	610	150
B3	0	1829	160	B9	0	1372	175	B15	6	610	150
B4	0	1829	160	B10	0	1372	175	B16	0	1372	160
B5	0	1829	160	B11	3.9	1372	160	B17	2.8	1372	160
B6	-4.7	1829	175	B12	-3.9	2438	175	B18		2133	160

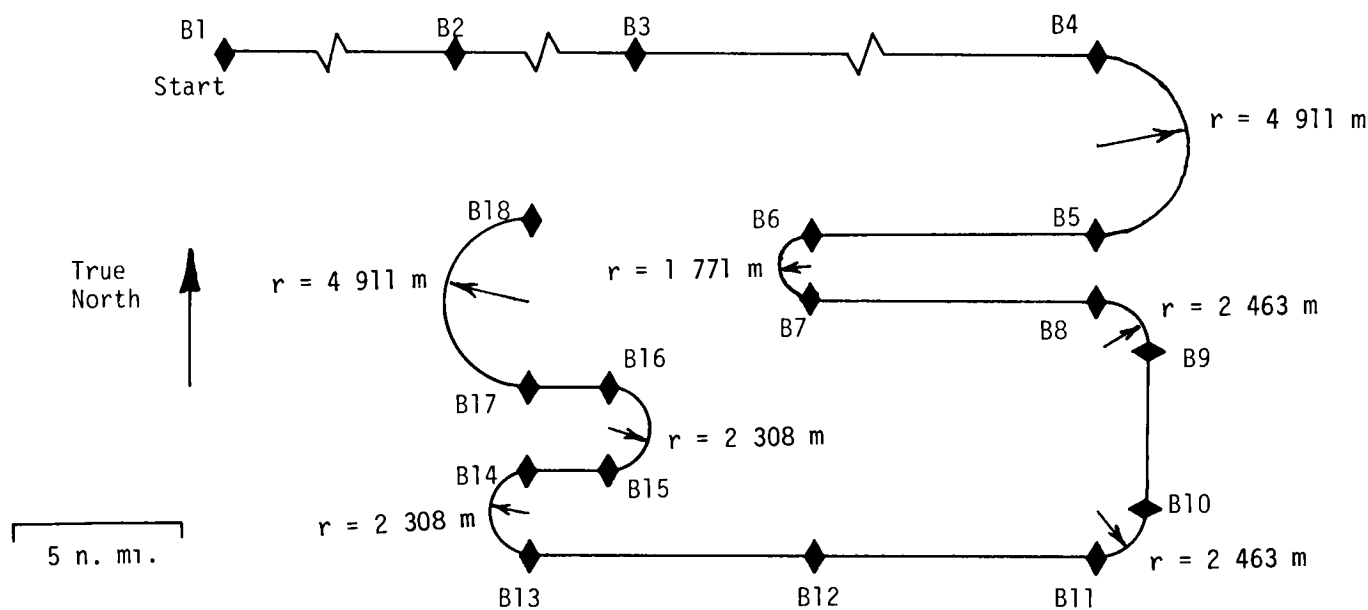


Figure 8.- Path B for tracking evaluation at airport-terminal-area speeds.

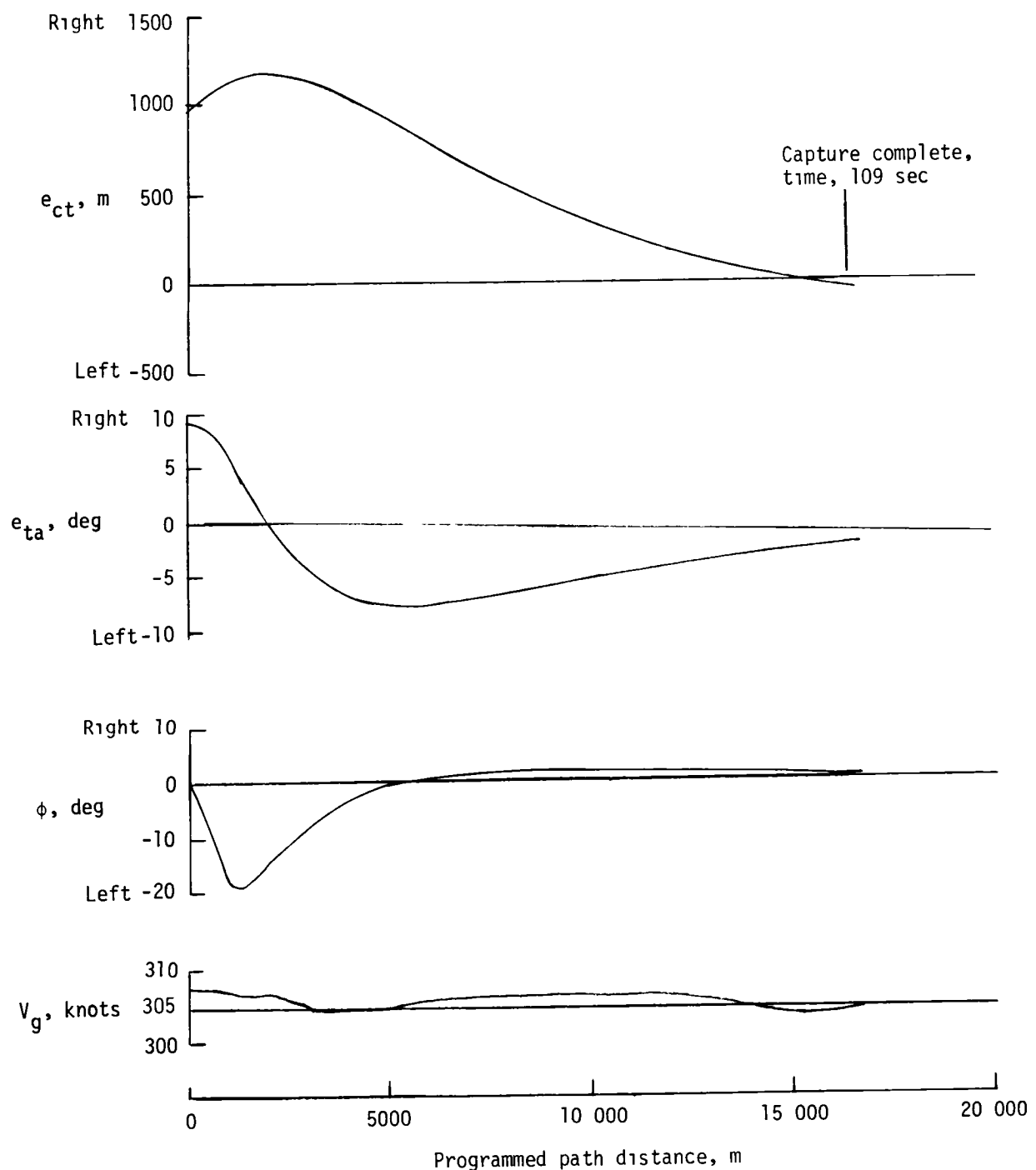


Figure 9.- First horizontal path capture test condition for high speed.

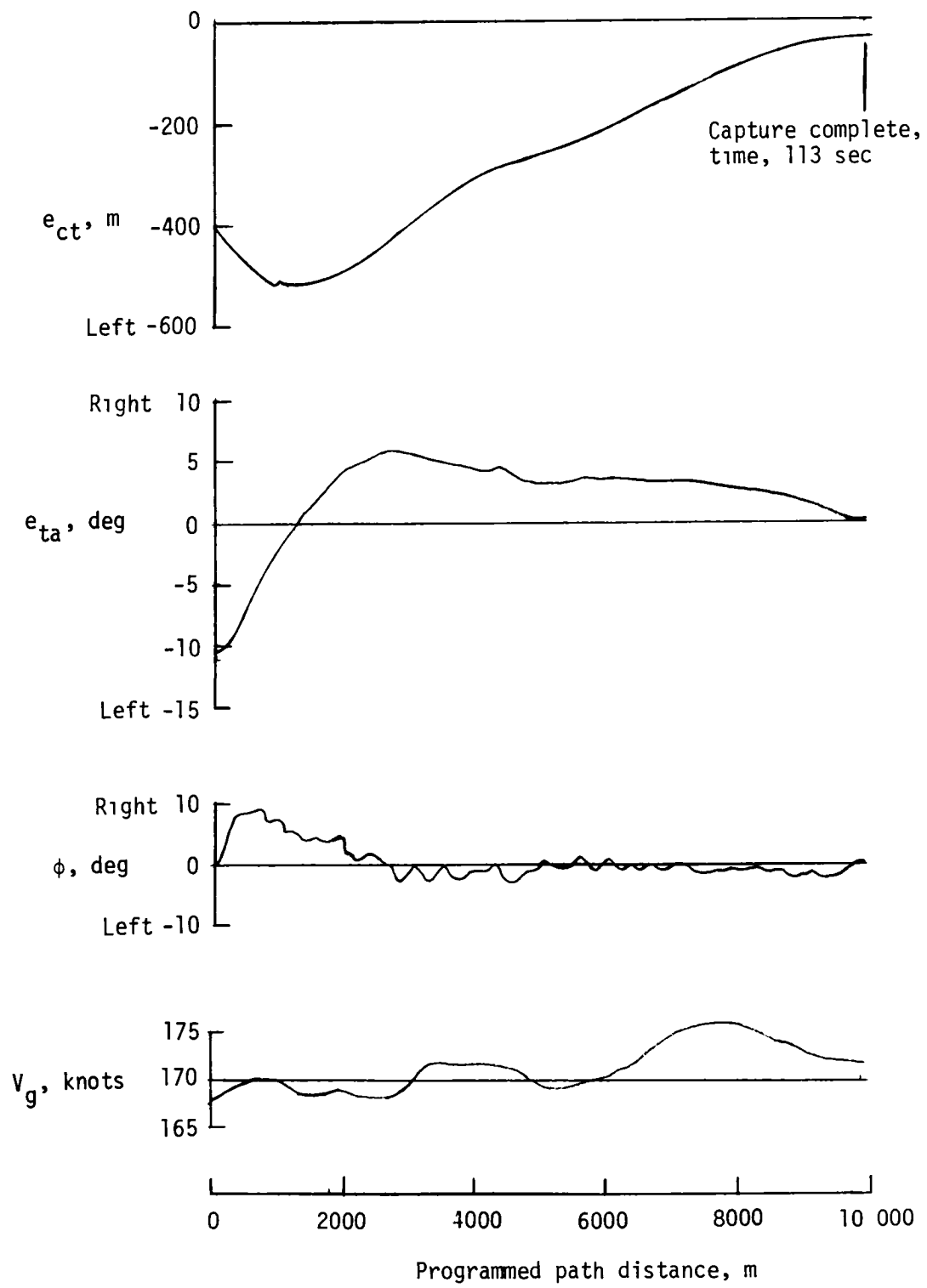


Figure 10.- First horizontal path capture test condition for low speed.

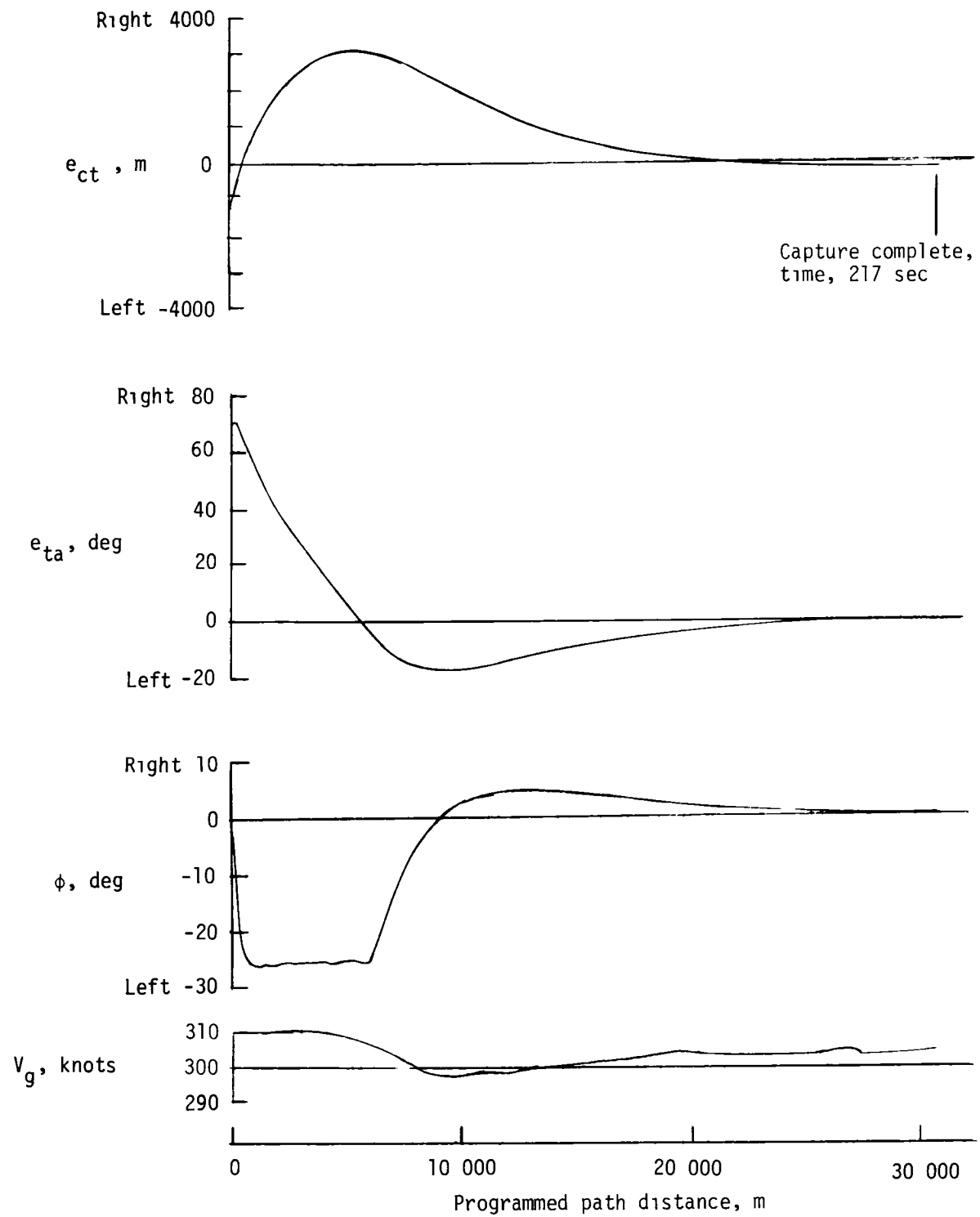


Figure 11.- Second horizontal path capture test condition for high speed.

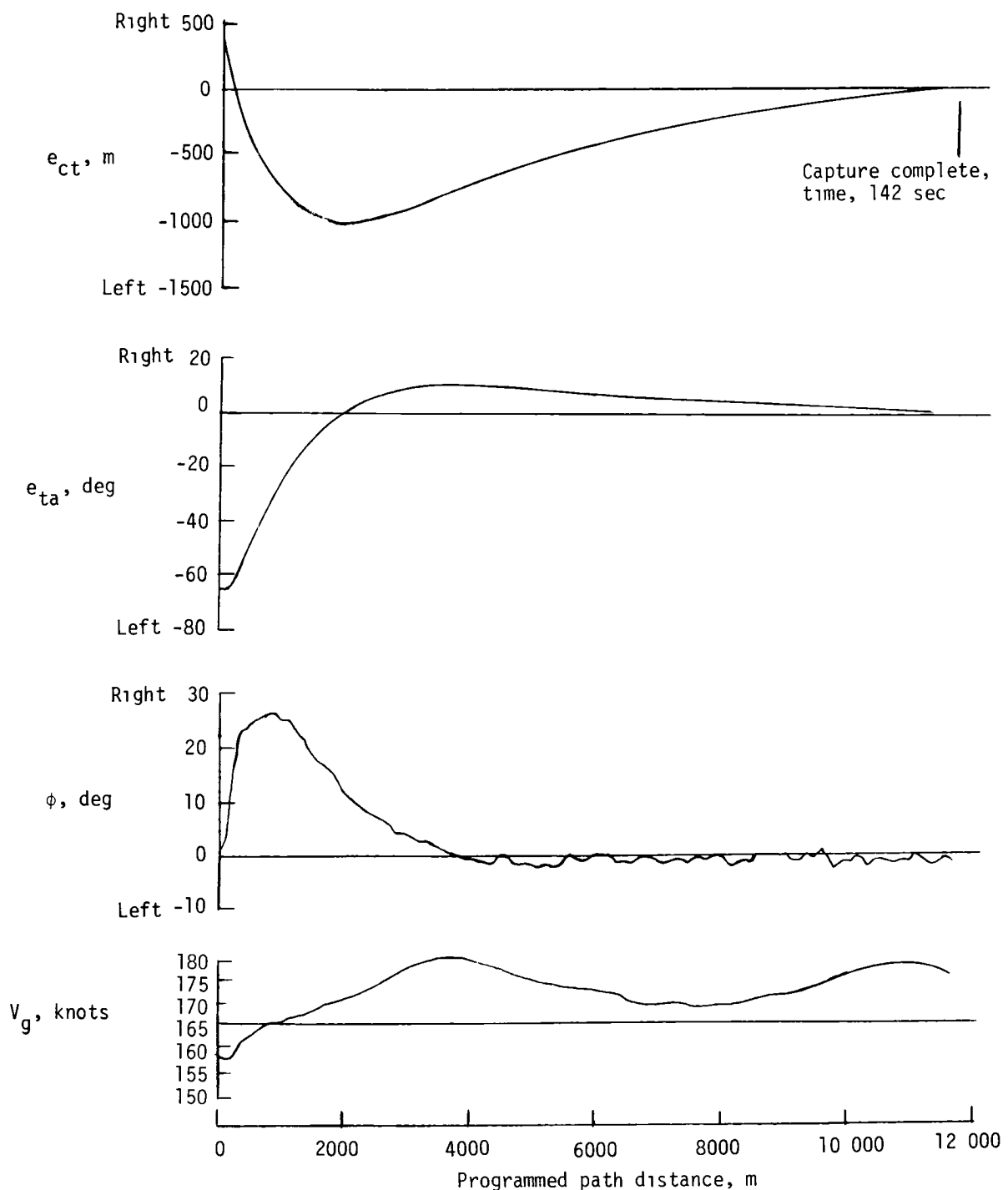


Figure 12.- Second horizontal path capture test condition for low speed.

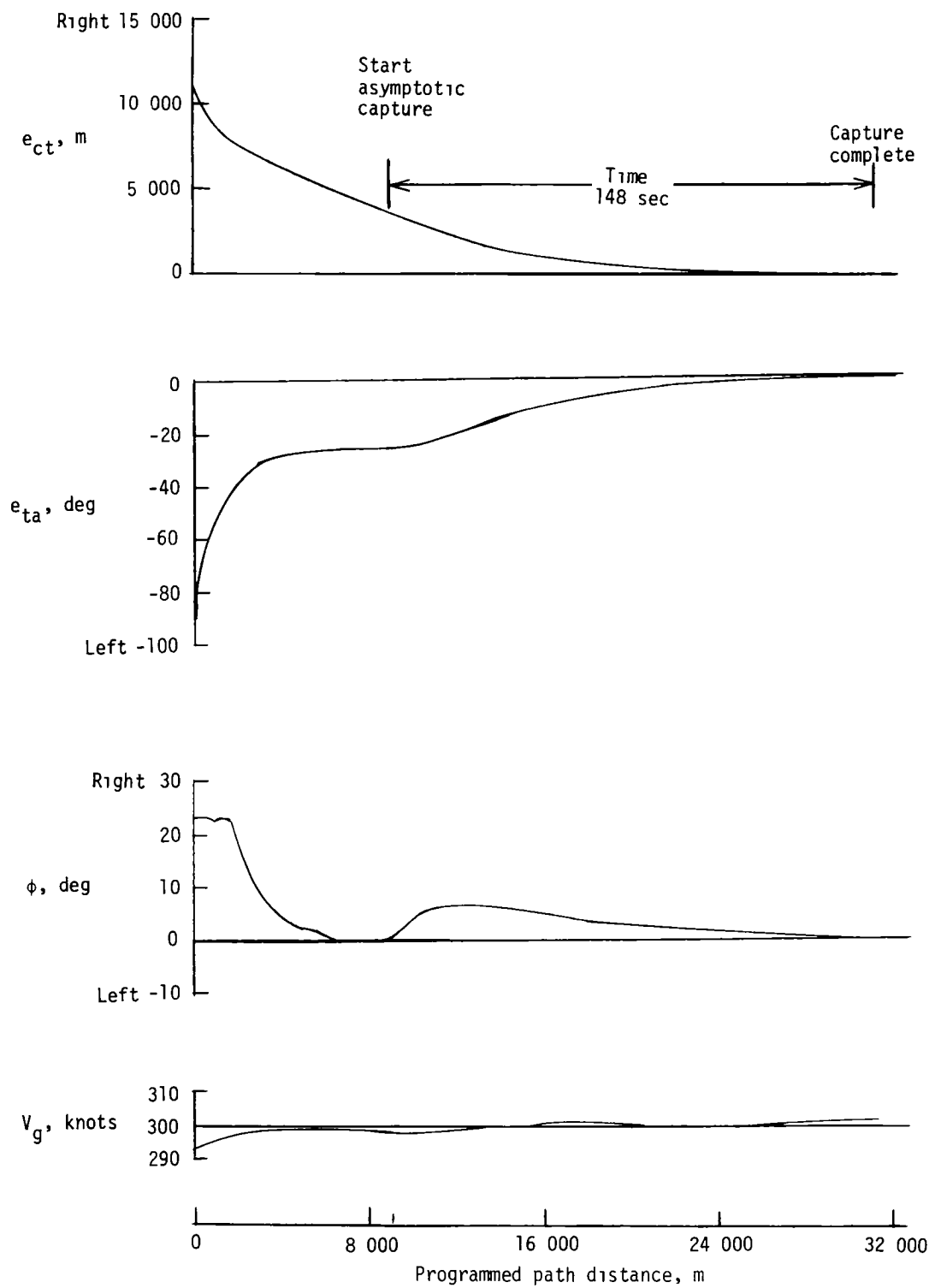


Figure 13.- Third horizontal path capture test condition for high speed.

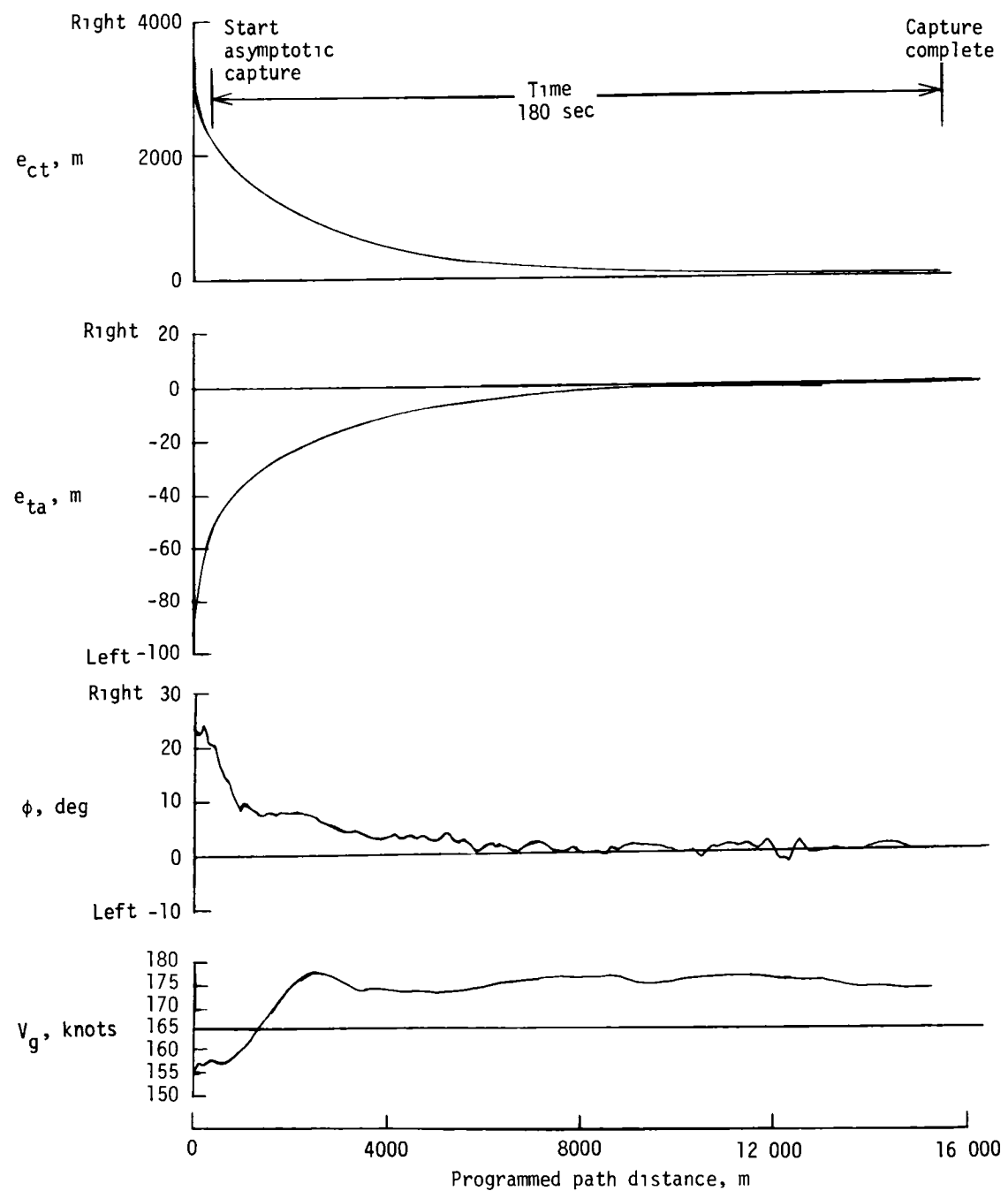


Figure 14.- Third horizontal path capture test condition for low speed.

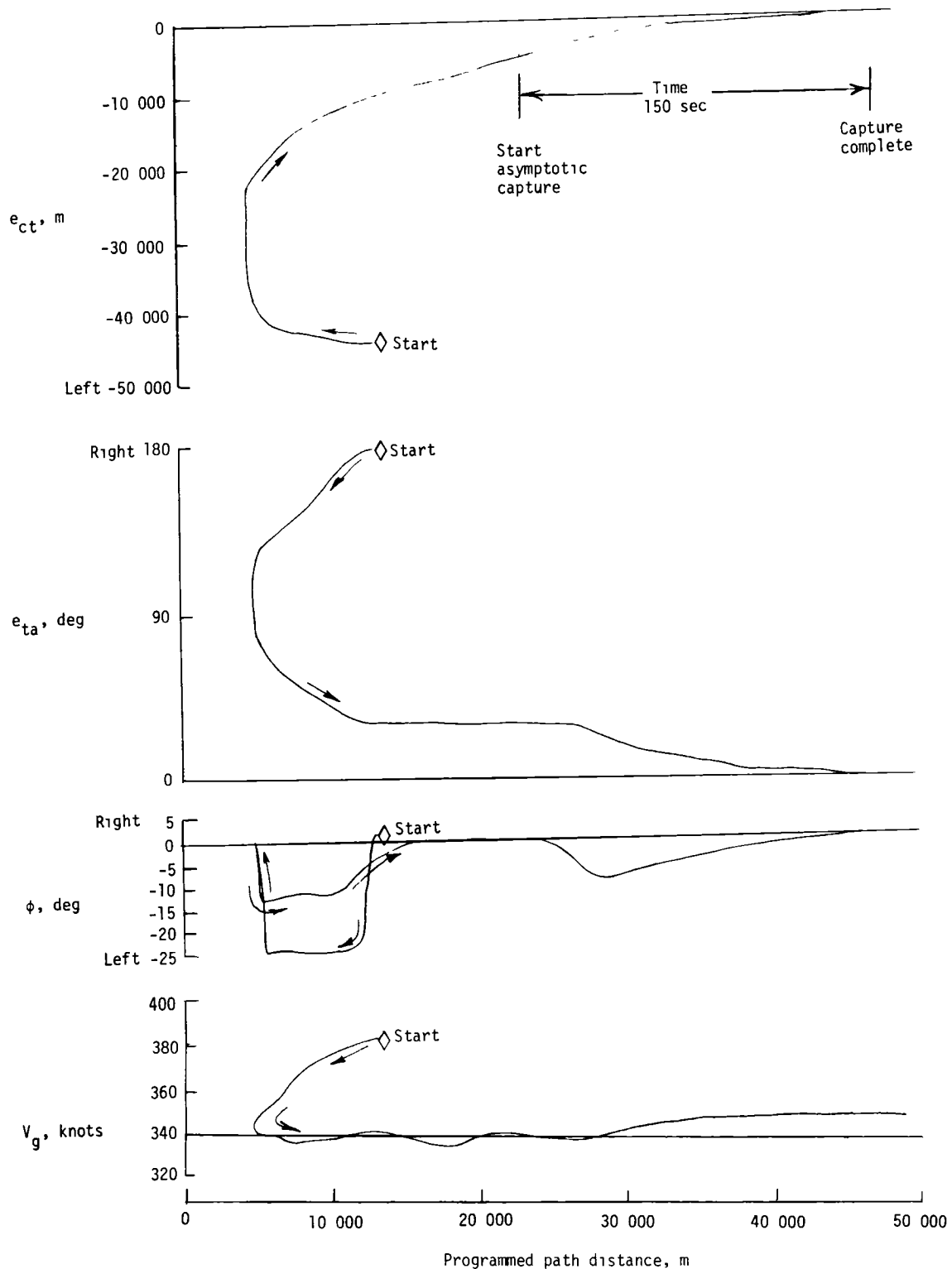


Figure 15.— Fourth horizontal path capture test condition for high speed.

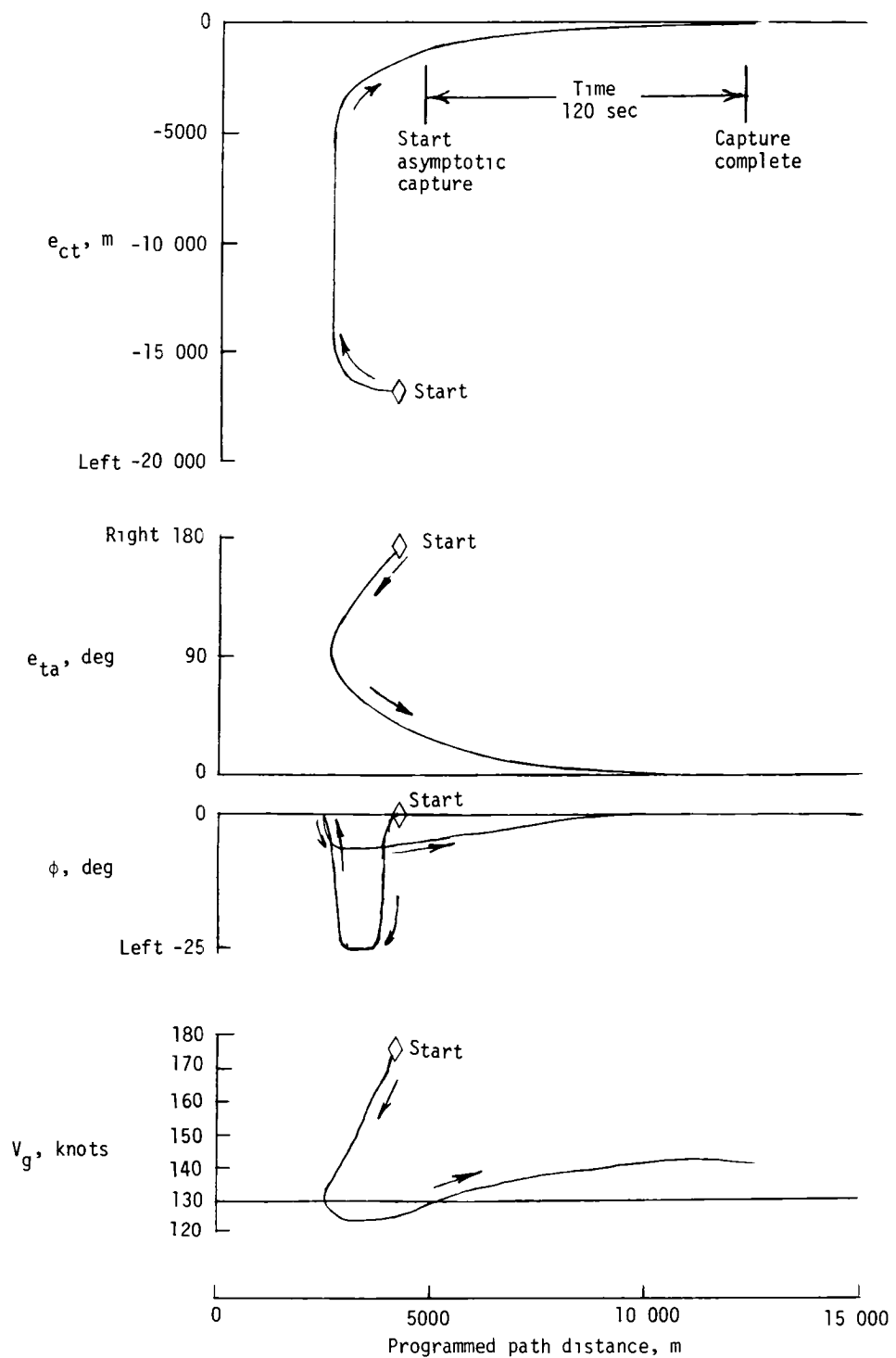


Figure 16.- Fourth horizontal path capture test condition for low speed.

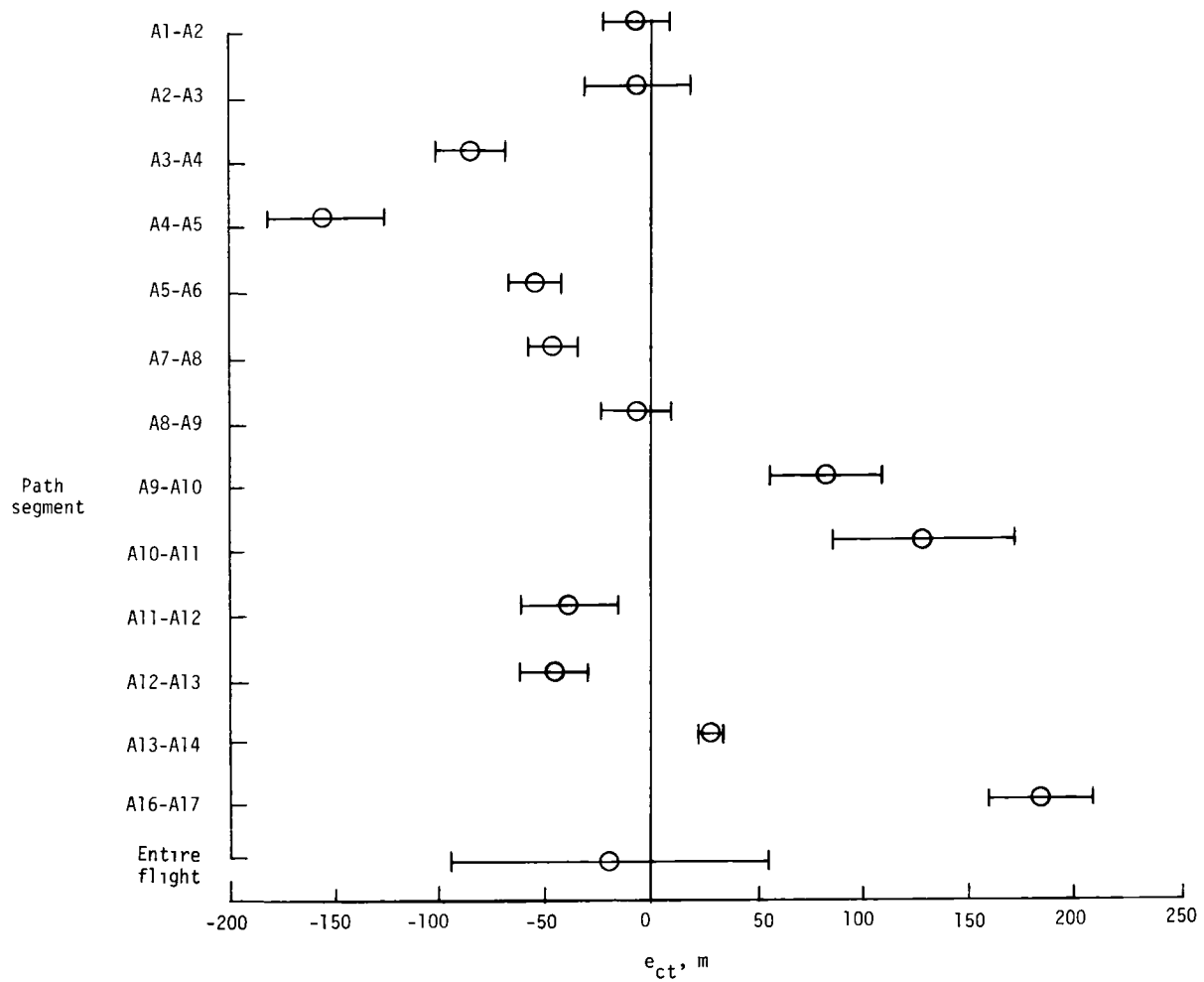


Figure 17.- Mean and standard deviation of cross-track error for flight on path A.

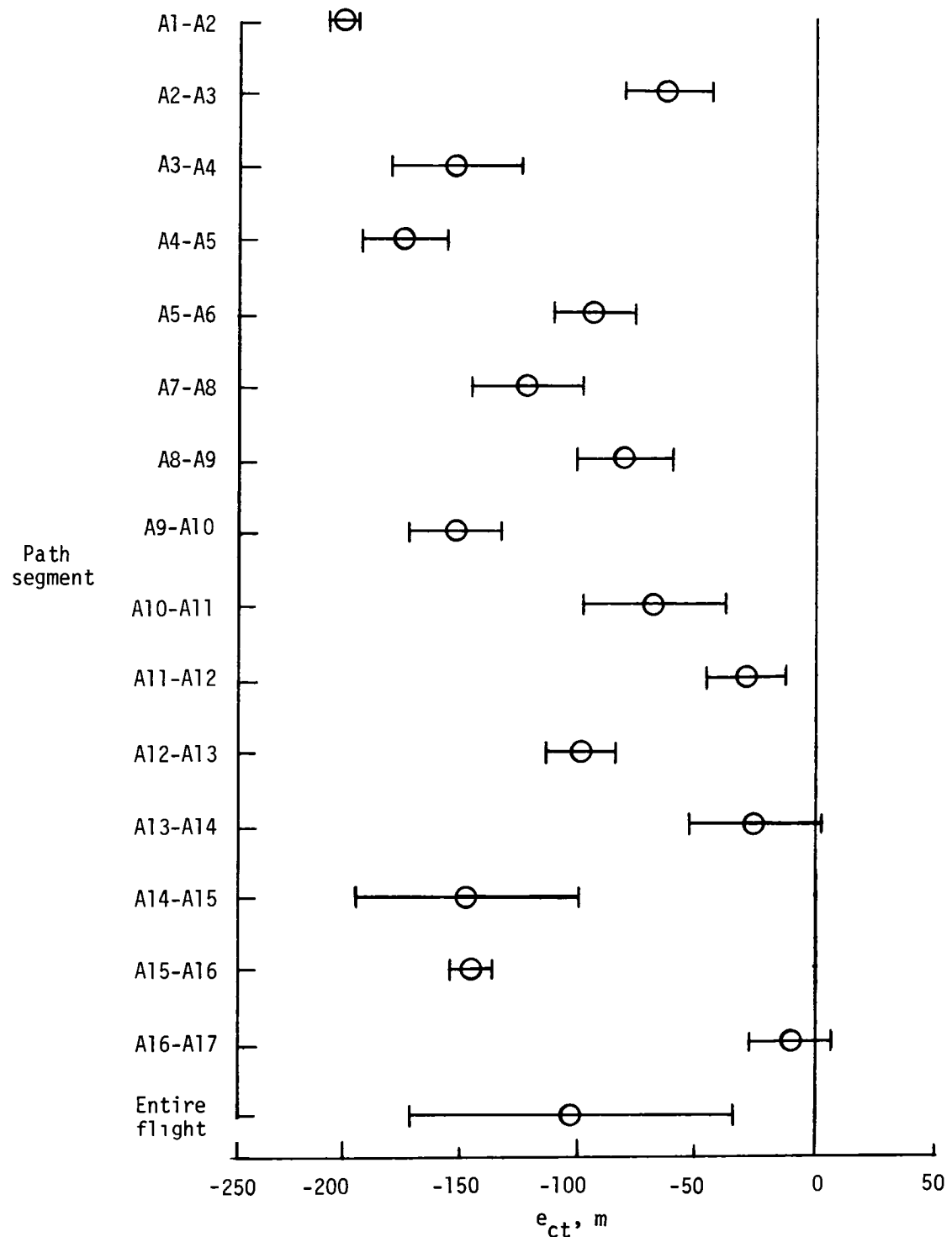


Figure 18.- Mean and standard deviation of cross-track error for flight 2 on path A.

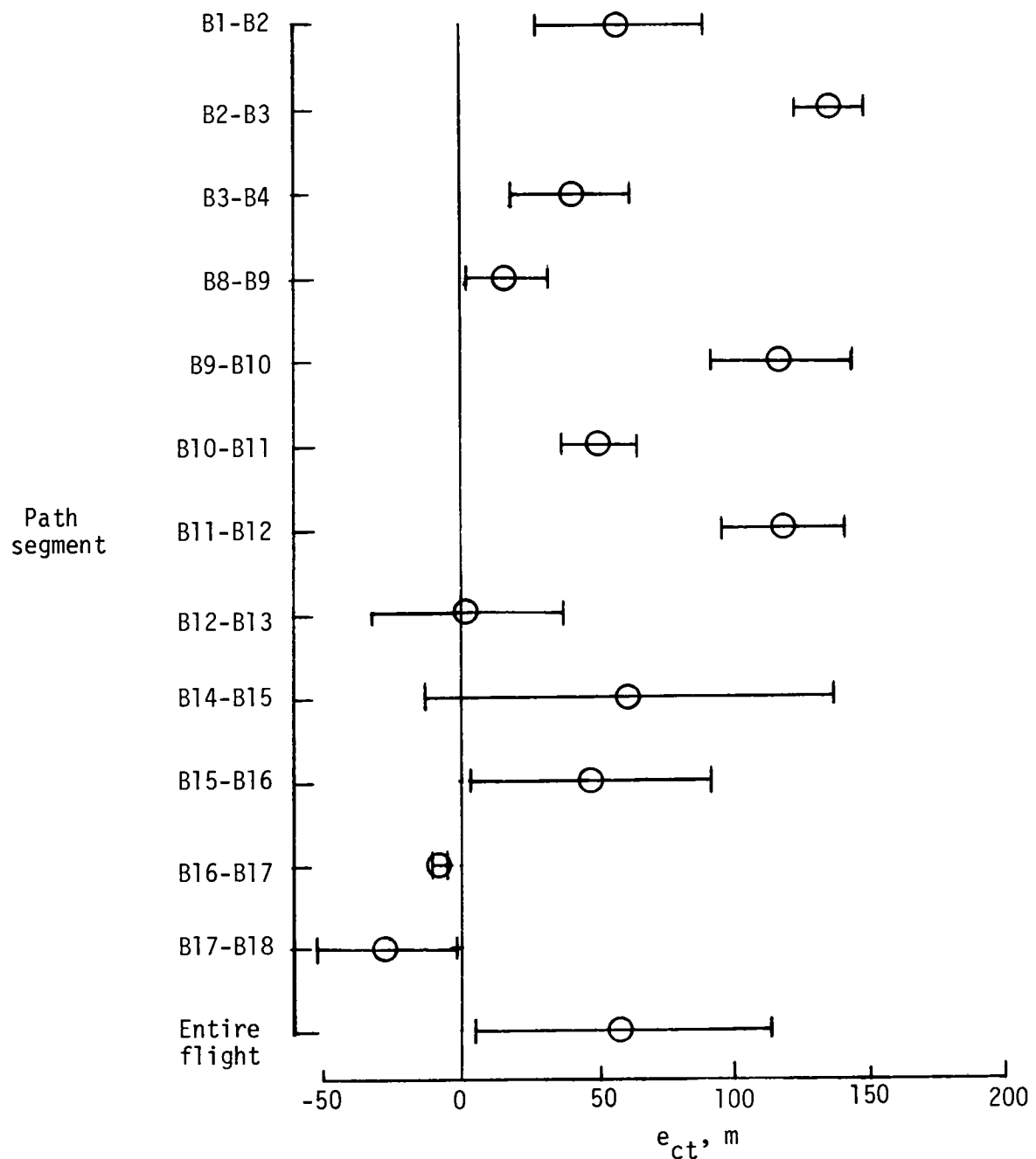


Figure 19.- Mean and standard deviation of cross-track error on path B.

**End of Document**